JOURNAL OF MAGNETIC RESONANCE **129,** 201–206 (1997)
ARTICLE NO. MN971259

COMMUNICATIONS

In Vivo Longitudinally Detected ESR Measurements at Microwave Regions of 300, 700, and 900 MHz in Rats Treated with a Nitroxide Radical

Hidekatsu Yokoyama,*[,1] Toshiyuki Sato,† Tateaki Ogata,‡ Hiroaki Ohya-Nishiguchi,* Hitoshi Kamada*

**Institute for Life Support Technology, Yamagata Technopolis Foundation, Yamagata 990, Japan; †Yamagata Research Institute of Technology, Yamagata 990, Japan; and ‡Faculty of Engineering, Yamagata University, Yonezawa 992, Japan*

Received March 19, 1997; revised August 22, 1997

A signal detector of longitudinally detected ESR (LODESR) is independent of the resonant frequency. We developed an *in vivo* LODESR spectrometer operating in the regions of 300, 700, and 900 MHz. Using this apparatus, we estimated signal intensities at different operating frequencies obtained from non- or high-dielectric loss phantoms that contained nitroxide radical solutions and from live rats that had received a nitroxide radical. Our result, higher signal intensities in the high-dielectric loss samples (such as physiological saline solution and animals) at a lower frequency, shows that the influence of a decrease in dielectric loss dominates over the signal reduction caused by smaller Zeeman splitting. We believe that this finding strongly supports an *in vivo* ESR resonant frequency that tends to be low.

Key Words: **LODESR; *in vivo* ESR; resonant frequency; dielectric loss; nitroxide radical.**

In recent years, *in vivo* ESR spectrometers for experimental animals (e.g., rat and mouse) have been developed and their designs improved remarkably (*1–4*), and their resonant frequencies tended to decrease (300–1000 MHz). First, an increase in the sample size necessitates the use of a large resonator, which needs to be operated at a sufficiently long wavelength. Second, to perform ESR measurements of large high-dielectric loss samples (such as living animals), one must apply lower frequency microwaves where the losses are sufficiently small. Approaching those lower frequencies (i.e., in the region 1000 to 300 MHz), ESR signal intensity will be reduced due to smaller Zeeman splitting. On the other hand, a reduction in dielectric loss in the lower frequency regions may compensate for this signal reduction. However, it is difficult to estimate signal intensities that are obtained from ESR measurements made in different operating frequency bands (such as the regions 300, 700, and 900 MHz) due to variations in the detectors for each band.

[1] To whom correspondence should be addressed.

We have been developing an *in vivo* longitudinally detected ESR (LODESR) system that operates at 700 MHz based on a bridged loop–gap resonator (BLGR) and a pair of saddle-type pickup coils (*5*). With a LODESR technique, the signal is derived from a longitudinal oscillation of the spin magnetization parallel to the *z* axis under on/off modulated ESR irradiation (*6, 7*). Thus a signal detector of LODESR is independent of the resonant frequency. If we fabricate some resonators with different resonant frequencies, we can estimate signal intensities obtained from LODESR measurements made at different operating frequencies by a single detector.

In this study, we apply the LODESR measurements to phantoms of a nitroxide radical in microwave regions of 300, 700, and 900 MHz. One phantom is a non-dielectric loss sample and another, a high-dielectric loss type (a model of the *in vivo* sample). We also measured LODESR signals from the heads of living rats that had received a nitroxide radical in the same microwave regions.

We fabricated three types of the BLGRs (*8*). The first is a four-gap type with interior and exterior bridge shields. This resonator was driven at a frequency of approximately 900 MHz (Fig. 1a). The second is a two-gap type with interior bridge shields, driven at a frequency of approximately 700 MHz (Fig. 1b). The third is a one-gap type with interior and exterior bridge shields, driven at a frequency of approximately 300 MHz (Fig. 1c). The loop size of all resonators is 10 mm in axial length and 43 mm in inner diameter. The bridge shield is located at the gap via a Teflon spacer that is 0.5 mm thick. It can reduce leakage of the electrical field from the gap (*8*).

The details of our LODESR system have been previously described (*5*). Its block diagram is shown in Fig. 2. For the main magnet, a commercially available electromagnet (modified RE3X, JEOL, Japan) was used. A supplementary Helmholtz coil was used as the field scan coil. The magnetic

1090-7807/97 $25.00

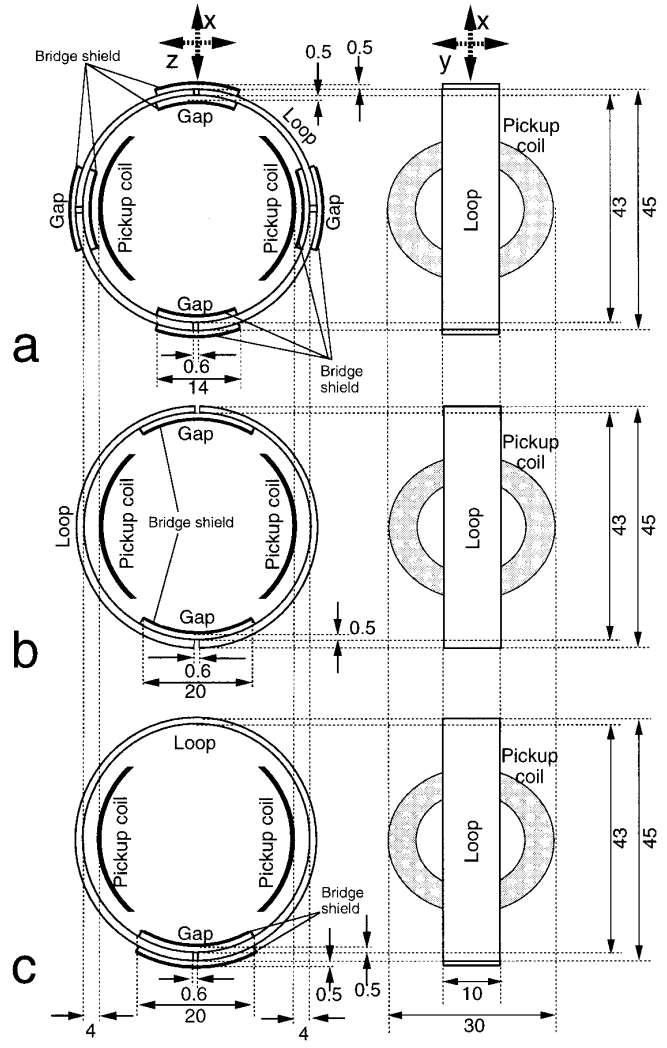

FIG. 1. Schema of an outer view of the BLGRs in the regions of 900 (a), 700 (b), and 300 (c) MHz. Dimensions are in mm.

field was scanned by controlling the current in the field scan coils at a maximum scan rate of 7.5 mT/s. The current supplied to the field scan coils was controlled by a personal computer (PC9821Xa13, NEC, Japan) via a D/A converter (DAJ98, Canopus Co., Ltd., Japan). The BLGRs were driven by oscillators (POS-400, 767, and 1025 for the regions 300, 700, and 900 MHz, respectively; Mini circuit, New York) and a power amplifier (A1000-1050, R&K, Japan; gain, 46 dB; max power, 50 W; bandwidth, 200–1000 MHz). The irradiation power was measured with a power meter (437B, Hewlett–Packard, Palo Alto; bandwidth, 0.1–18 GHz). The on/off modulation of the microwaves was operated by using a pin switch (ZYSWA, Mini circuit, New York; bandwidth, DC-5000 MHz; isolation, 27 dB; switching time, 5 ns) at a modulation frequency of 1 MHz.

The detection system consists of a pair of pickup coils placed inside the BLGR, a preamplifier, and a lock-in amplifier. The LODESR measurements in the regions 300, 700, and 900 MHz are made by this one detection system. The pickup coil is a saddle-type coil (30 mm in outer diameter)

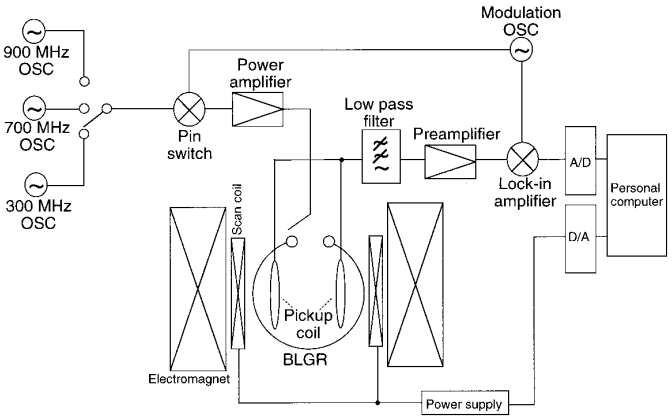

FIG. 2. Block diagram of our LODESR system.

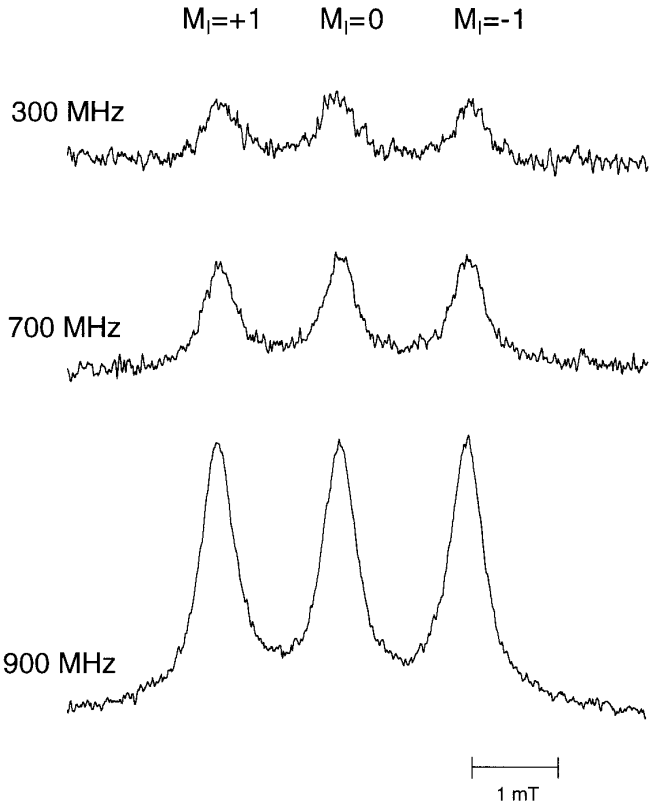

FIG. 3. Examples of the LODESR spectra in the regions of 300, 700, and 900 MHz obtained from the non-dielectric loss phantom. This phantom is a sample tube that contained 15 ml of a 1 mM solution of carbamoyl-PROXYL dissolved in benzene. The instrument settings are microwave average power, 16 W; microwave frequency, 296, 663, or 883 MHz; scan rate, 5 mT/s; accumulation number, 16; modulation frequency, 1 MHz; time constant, 1 ms.

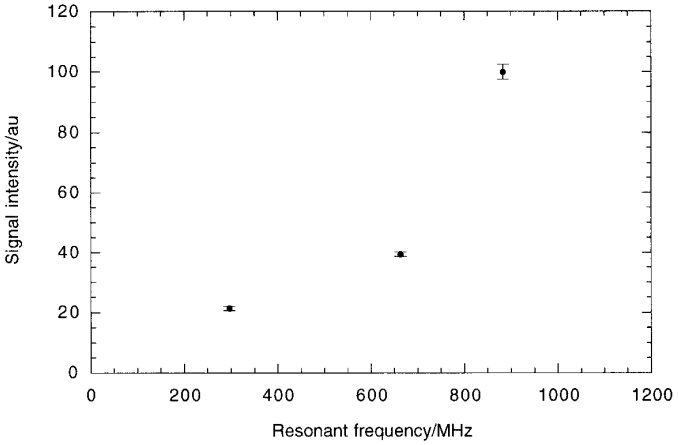

FIG. 4. The signal intensities of the non-dielectric loss phantom plotted against the resonant frequency (values are means ± standard error from four independent determinations).

which is constructed from 15 turns of copper wire (0.3 mm in diameter). The distance between the pickup coils and inner surface of the loop is 4 mm (Figs. 1a–1c). The signal induced in the pickup coils by the longitudinal oscillation of the spin magnetization is amplified by a preamplifier (SA-430F5, NF Electronic Instruments, Japan; noise figure, 0.6 dB; gain, 46 dB; bandwidth, 0.001–100 MHz), followed by detection, using a lock-in amplifier (5302, PARC, Princeton; bandwidth, 1 mHz–1 MHz) at the modulation frequency. The internal oscillator of the lock-in amplifier is used as the modulation/reference signal source. To avoid rectifying the modulated microwave, a low-pass filter (cutoff frequency, 10 MHz) is connected between the pickup coils and the preamplifier. The LODESR spectral data are collected via an A/D converter (ADJ98, Canopus Co., Ltd., Japan), using a personal computer.

In this study, the unloaded Q is defined as the Q factor of the resonator with pickup coils only, and the loaded Q is defined as the Q factor with pickup coils and a sample. For the 300-, 700-, or 900-MHz region, the unloaded Q of the BLGR was 160, 150, or 230, respectively. The distance between the gap and bridge shield (0.5 mm) is sufficiently smaller than that between the gap and pickup coil (4 mm). Furthermore, the magnetic field of the resonator (B_1) does not penetrate the pickup coils (Figs. 1a–1c). Therefore the isolation between the resonator and the pickup coils is excellent. LODESR measurements are made in the best coupling with the sample by minimizing reflected power from the resonator, which is monitored by an internal power meter of the power amplifier.

We already found that the detection of LODESR signals is barely affected by the variation in resonant properties as opposed to the detection of a conventional ESR (*5*). Thus the sensitivity of *in vivo* LODESR measurements is barely reduced when the resonant properties are perturbed by the physiological motion of living animals.

A nitroxide radical, 3-carbamoyl-2,2,5,5-tetramethylpyrrolidine-1-oxyl (carbamoyl-PROXYL, Aldrich Chemical Co., Ltd., Milwaukee), was used. Fifteen milliliters of a 1 mM solution of carbamoyl-PROXYL that had been dissolved in benzene was placed in a sample tube (25 mm in inner diameter, 31 mm in axial length) for use as the non-dielectric loss phantom. The same amount of a 1 mM solution of carbamoyl-PROXYL dissolved in a physiological saline solution (0.9% sodium chloride aqueous solution) was placed in another sample tube (of identical size) to be used as the high-dielectric loss phantom. Each phantom was

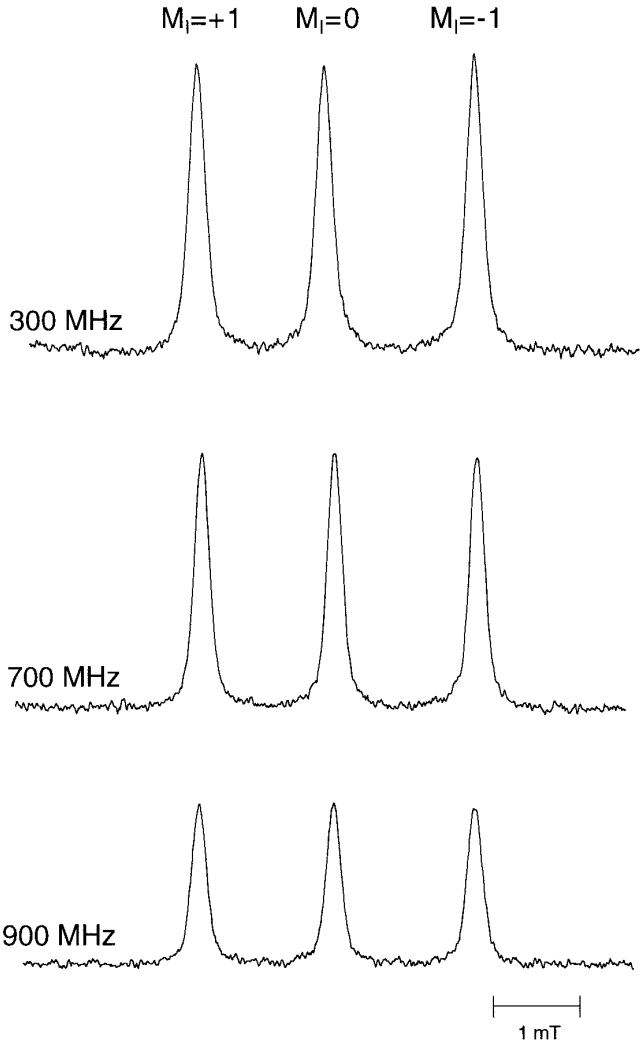

FIG. 5. Examples of the LODESR spectra in the regions of 300, 700, and 900 MHz obtained from the high-dielectric loss phantom. This phantom is a sample tube that contained 15 ml of a 1 mM solution of carbamoyl-PROXYL dissolved in a physiological saline solution. The instrument settings are microwave average power, 16 W; microwave frequency, 296, 698, or 988 MHz; scan rate, 5 mT/s; accumulation number, 16; modulation frequency, 1 MHz; time constant, 1 ms.

placed at the center of the BLGR. The filling factor was about 0.3 (*9*). In the 300-, 700-, or 900-MHz region, the loaded Q factors for the non-dielectric loss and high-dielectric loss phantom were 130, 150, or 220, and 65, 55, or 30, respectively. LODESR measurements were performed at an average power of 16 W at operating frequencies of 296, 663, and 883 MHz (non-dielectric loss phantom) or 296, 698, and 988 MHz (high-dielectric loss phantom). The signal intensity of carbamoyl-PROXYL was derived from the peak height of the lowest component ($M_I = +1$) of the triplet spectrum. To correct for variations in the Q factor of resonators, the signal intensity that had been obtained was normalized by employing the equation (see Appendix 1)

$$S_N = S_0/(1 + Q_L/Q_N - Q_L/Q_U),$$

where S_N is the normalized signal intensity, S_0 is the signal intensity obtained from measurement, Q_U is the unloaded Q, Q_L is the loaded Q, and Q_N is the normalized unloaded Q. In this study, we used a value of 200 for Q_N: so we obtained the normalized signal intensity that had been predicted from using a $Q = 200$ resonator.

Figure 3 shows examples of the LODESR spectra obtained from the non-dielectric loss phantom in the three bands. Their peak heights were corrected by the above-mentioned method. The signal-to-noise ratios (SNRs) were about 4, 8, and 30, in the regions of 300, 700, and 900 MHz, respectively. Figure 4 shows the signal intensities of the non-dielectric loss phantom plotted against the resonant frequency. Here the signal intensities are lower as the frequency is reduced (values are means ± standard error from four independent determinations).

Figure 5 shows examples of the spectra of the high-dielectric loss phantom in the regions of 300, 700, and 900 MHz.

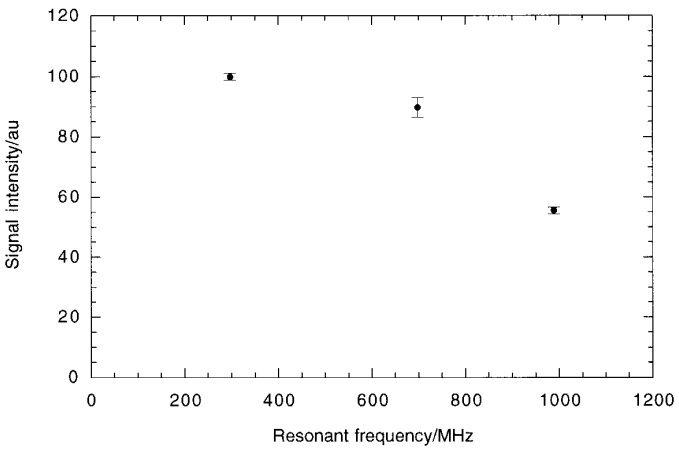

FIG. 6. The signal intensities of the high-dielectric loss phantom plotted against the resonant frequency (values are means ± standard error from four independent determinations).

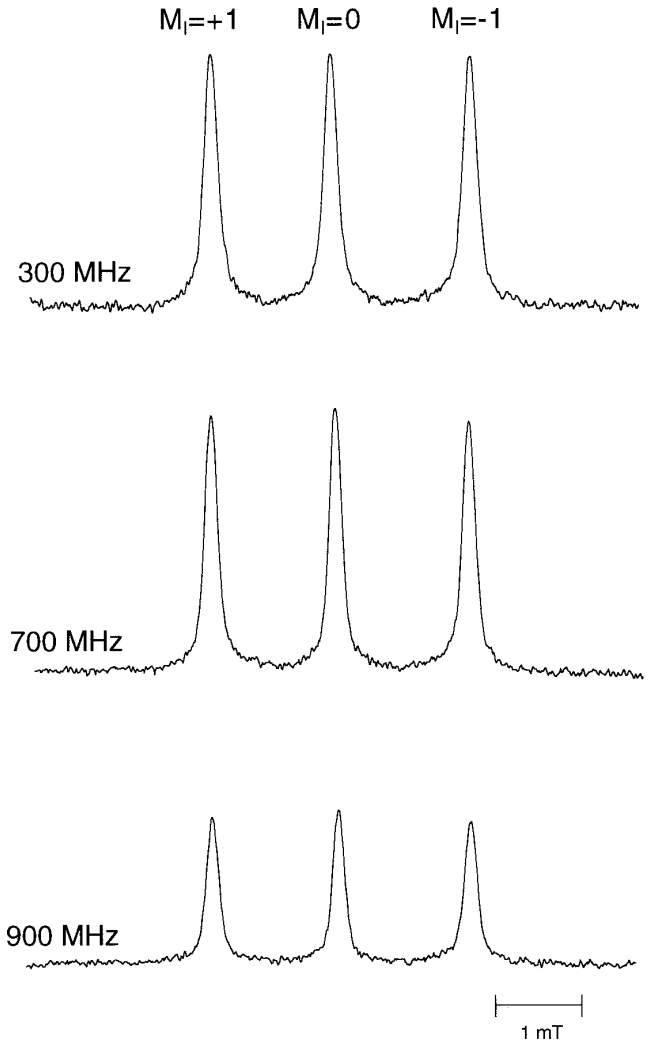

FIG. 7. Examples of the LODESR spectra in the regions of 300, 700, and 900 MHz obtained from the heads of rats that had received 5 ml of 0.2 M carbamoyl-PROXYL via intraperitoneal route. The instrument settings are microwave average power, 8 W; microwave frequency, 296, 675, or 955 MHz; scan rate, 5 mT/s; accumulation number, 16; modulation frequency, 1 MHz; time constant, 1 ms.

The SNRs are about 50, 50, and 30, respectively. Figure 6 shows signal intensities of the high-dielectric loss phantom plotted against the resonant frequency. The signal intensities in the 700-MHz region are much higher than those in the 900 MHz region; and those in the 300-MHz region are slightly higher when compared to those in the 700-MHz region.

At lower resonant frequencies, both Zeeman splitting and the dielectric loss become smaller. Smaller Zeeman splitting reduces the signal intensity, but a smaller dielectric loss increases it. The result with the non-dielectric loss phantom reflects the frequency characteristic of Zeeman splitting; on the other hand, the result with the high-dielectric loss phantom reflects a combination of the frequency characteristic

of Zeeman splitting and that of the dielectric loss. Therefore these findings suggest that the influence of the dielectric loss dominates that of Zeeman splitting at a lower resonant frequency.

The male Wistar rats (each weighing 200 g) were divided into three groups for measurement at 300 ($n = 5$), 700 ($n = 5$), and 900 ($n = 5$) MHz. Carbamoyl-PROXYL was dissolved in a physiological saline solution at 0.2 M. The animals received 5 ml (1 mmol) of the carbamoyl-PROXYL solution via intraperitoneal route. Ten minutes after the injection and under pentobarbital anesthesia, each animal was restrained in the spectrometer, with its interaural line aligned 10 mm posterior to the center of the BLGR. The loaded Q was 60, 60, or 20 at 300, 700, or 900 MHz, respectively. LODESR measurements were made at an operating frequency of 300, 678, and 955 MHz and an average power of 8 W. The signal intensity was normalized as described above.

Figure 7 shows examples of the LODESR spectra in the three bands obtained from the rats' heads after the intraperitoneal injection of nitroxide radical. The SNRs were about 50, 50, and 30, in the 300-, 700-, and 900-MHz regions, respectively. Figure 8 shows the signal intensities obtained at the heads of the rats plotted against the resonant frequency. Variation in the signal intensities between animals is larger than that obtained with phantom experiments. The signal intensities in the 700-MHz region are much higher than those in the 900-MHz region; and those in the 300-MHz region are slightly high when compared to those in the 700-MHz region. This relationship between signal intensities and resonant frequency is similar in the high-dielectric loss phantom, suggesting that the sample tube which contains nitroxide dissolved in the physiological saline solution functions sufficiently as the phantom of a living body. This result also shows that in the *in vivo* LODESR measurements at lower

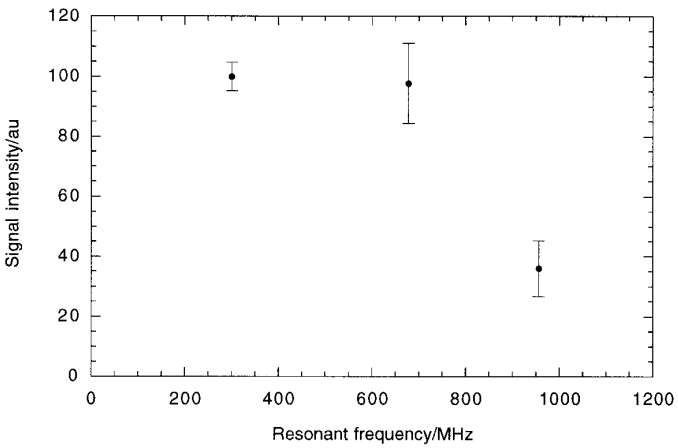

FIG. 8. The signal intensities from the heads of the nitroxide-treated rats plotted against the resonant frequency (values are means ± standard error; $n = 5$ for each frequency region).

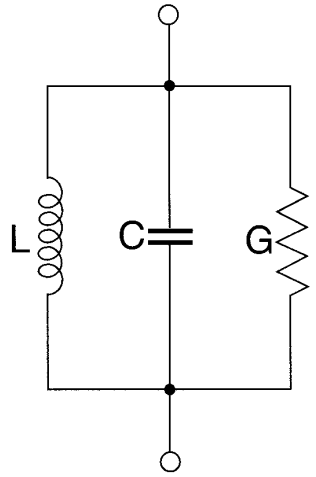

FIG. 9. An equivalent circuit of the BLGR. L, inductance of a loop; C, total capacitance formed by the gaps and bridge shields; G, total conductance of the resonator.

frequencies, the influence of a reduction in the dielectric loss dominates over the signal reduction caused by smaller Zeeman splitting, as in the measurement taken with the high-dielectric loss phantom.

The energy dissipation in the rat is roughly estimated to be about 4, 5, and 7 W at 300, 700, and 900 MHz, respectively, on the basis of the change in the resonator Q after loading (see Appendix 2). This indicates that invasive damages by heat is least in the 300-MHz region.

In summary, this work presents a LODESR spectrometer operating in the regions of 300, 700, and 900 MHz. Using this apparatus, we analyzed the LODESR signal obtained from non-or high-dielectric loss phantoms that contained nitroxide radical solutions and from live rats that had received a nitroxide radical. Our result, higher signal intensities in the high-dielectric loss samples (such as physiological saline solution and animals) at a lower frequency (i.e., in the 300-MHz region), shows that the influence of a decrease in dielectric loss dominates over the signal reduction caused by smaller Zeeman splitting. Furthermore, the energy dissipation in the sample (i.e., heat damage) was smaller at a lower frequency. Thus, a low-frequency LODESR is suitable for *in vivo* analysis. We believe that the results of the present study strongly support an *in vivo* ESR resonant frequency that tends to be low.

APPENDIX 1

In an equivalent circuit of the BLGR (as shown in Fig. 9), the unloaded Q (Q_U), loaded Q (Q_L), normalized unloaded Q (Q_N), and normalized loaded Q (Q_X) are defined as

$$Q_U = 1/(G_0 L\omega_0), \qquad [1]$$

$$Q_L = 1/((G_0 + G_1)L\omega_0), \quad [2]$$

$$Q_N = 1/(G_0'L\omega_0), \quad [3]$$

$$Q_X = 1/((G_0' + G_1)L\omega_0), \quad [4]$$

where G_0 is the unloaded conductance, $G_0 + G_1$ is the loaded conductance, G_0' is the normalized G_0, L is the inductance of the loop conductor, and ω_0 is the resonant frequency.

Equations [1] and [2] give

$$G_1 = (1/Q_L - 1/Q_U)/L\omega_0 \quad [5]$$

and, Eq. [3] gives

$$G_0' = (1/Q_N)/L\omega_0. \quad [6]$$

With Eqs. [4], [5], and [6],

$$Q_X = 1/(1/Q_L - 1/Q_U + 1/Q_N) \quad [7]$$

is valid.

Because the signal intensity is proportional to Q (*10*), we have

$$S_N = S_0(Q_X/Q_L), \quad [8]$$

where S_N is the normalized signal intensity, and S_0 is the signal intensity obtained from measurement.

With Eq. [7], Eq.[8] is transformed into

$$S_N = S_0/(1 + Q_L/Q_N - Q_L/Q_U) \quad [9]$$

as given by the equation in the text.

APPENDIX 2

In an equivalent circuit of the BLGR (as shown in Fig. 9), the unloaded Q (Q_U) and loaded Q (Q_L) are defined as

$$Q_U = 1/(G_0L\omega_0), \quad [10]$$

$$Q_L = 1/((G_0 + G_1)L\omega_0), \quad [11]$$

where G_0 is the unloaded conductance, $G_0 + G_1$ is the loaded conductance, L is the inductance of the loop conductor, and ω_0 is the resonant frequency.

Equation [10] by Eq. [11] gives

$$G_1 = (Q_U/Q_L - 1)G_0. \quad [12]$$

Because G_0 and G_1 are in parallel,

$$G_1/G_0 = W_1/W_0, \quad [13]$$

where W_0 is the power dissipated by G_0 and W_1 is the power dissipated by G_1, is valid.

With Eq. [13], Eq. [12] gives

$$W_1 = (Q_U/Q_L - 1)W_0. \quad [14]$$

When irradiation power is defined as W_t,

$$W_t = W_0 + W_1 \quad [15]$$

is valid.

With Eq. [15], Eq. [14] is transformed into

$$W_1 = (1 - Q_L/Q_U)W_t. \quad [16]$$

W_1 is thought to be energy dissipation in the sample.

REFERENCES

1. L. J. Berliner and H. Fujii, *Science* **227,** 517 (1984).
2. S. Ishida, S. Matsumoto, H. Yokoyama, N. Mori, H. Kumashiro, N. Tsuchihashi, T. Ogata, M. Yamada, M. Ono, T. Kitajima, H. Kamada, and E. Yoshida, *Magn. Reson. Imaging* **10,** 21 (1992).
3. V. Quaresima, M. Alecci, M. Ferrari, and A. Sotgiu, *Biochem. Biophys. Res. Commun.* **183,** 829 (1992).
4. H. Yokoyama, T. Ogata, N. Tsuchihashi, M. Hiramatsu, and N. Mori, *Magn. Reson. Imaging* **14,** 559 (1996).
5. H. Yokoyama, T. Sato, N. Tsuchihashi, T. Ogata, H. Ohya-Nishiguchi, and H. Kamada, *Magn. Reson. Imaging* **15,** 701 (1997).
6. I. Nicholson, F. J. L. Robb, and D. J. Lurie, *J. Magn. Reson. B* **104,** 284 (1994).
7. A. Colligiani, D. Leporini, M. Lucchesi, and M. Martnelli, *in* ''Electron Magnetic Resonance of Disorder Systems'' (N. D. Yordanov, Ed.), pp. 16–37, World Scientific, Singapore (1991).
8. H. Hirata and M. Ono, *Rev. Sci. Instrum.* **67,** 1 (1996).
9. M. Ono, T. Ogata, K. Hsieh, M. Suzuki, E. Yoshida, and H. Kamada, *Chem. Lett.,* 491 (1986).
10. F. Bloch, *Phys. Rev.* **70,** 460 (1946).